Acta Biochim Biophys Sin 2023, 55(9): 1445–1455
https://doi.org/10.3724/abbs.2023079
Advance Access Publication Date: 17 August 2023
Original Article

Original Article

MFAP2 promotes the progression of oral squamous cell carcinoma by activating the Wnt/β-catenin signaling pathway through autophagy

Hao Zhang[1,2], Si Shen[1,2], Chong Feng[1,2], Gang Chen[2,*], and Xinxing Wang[1,*]

[1]Tianjin Institute of Environmental and Operational Medicine, Tianjin 300050, China, and [2]School and Hospital of Stomatology, Tianjin Medical University, Tianjin 300070, China

*Correspondence address. Tel: +86-22-84655206; E-mail: wxxemail@sina.cn (X.W.) / Tel: +86-22-83336767; E-mail: doctorchen@tmu.edu.cn (G.C.)

Received 7 December 2022 Accepted 23 March 2023

Abstract

Microfibrillar-associated protein 2 (MFAP2) is a small glycoprotein that is involved in vascular development and metabolic disease. The present study aims to explore the regulatory role of MFAP2 in the development and progression of oral squamous cell carcinoma (OSCC), including the underlying mechanisms. MFAP2 expression and its association with the progression of OSCC are explored using bioinformatics. MFAP2 expression in OSCC tissues is detected by immunohistochemical staining. SCC15 cell migration, invasion, apoptosis, proliferation, and viability are detected by wound healing, Transwell, flow cytometry, colony formation, and cell counting kit-8 assays. An *in vivo* experiment is used to detect tumor formation. Western blot analysis is used to determine MFAP2's regulatory role in autophagy and the Wnt/β-catenin signaling pathway. MFAP2 is highly expressed in SCC15 cells and OSCC tissues, which correlates positively with the poor prognosis of patients with OSCCs. Functionally, MFAP2 promotes oncogenic autophagy to increase cell invasion, migration, and proliferation but inhibits apoptosis in SCC15 cells and promotes tumor growth *in vivo*. Mechanistically, MFAP2 upregulates autophagy and Wnt/β-catenin signaling to stimulate OSCC development. Intriguingly, regulation of Wnt/β-catenin signaling dependent on autophagy contributes to the malignant behaviors of SCC15 cells. MFAP2 could serve as a novel biomarker for OSCC and could affect OSCC tumorigenesis and development via autophagic regulation of Wnt/β-catenin signaling.

Key words oral squamous cell carcinoma, microfibrillar-associated protein 2, autophagy, Wnt/β-catenin pathway, *in vivo*

Introduction

Oral squamous cell carcinoma (OSCC) is the most common malignant tumors of the oral cavity, accounting for approximately 90% of oral malignancies [1]. High mortality and high recurrence rates characterize OSCC, and its five-year overall survival (OS) rate is low, contributing to many deaths annually [2]. Most patients with OSCC die from postoperative recurrence caused by the high invasion and metastatic abilities of OSCC cells. Although advances in early diagnosis and combination treatment have significantly improved the mortality rate of patients with OSCC, the five-year survival rate for patients with OSCC remains low [3]. Thus, it is necessary to further explore the molecular mechanisms of invasion and metastasis in OSCC.

Microfibrillar-associated proteins (MFAPs) are extracellular matrix (ECM) glycoproteins that play an important role in the construction of microfibrils and tissue homeostasis. The MFAP family comprises MFAP1, MFAP2, MFAP3, MFAP4, and MFAP5, which are expressed in various human tissues and play diverse roles in physiological and pathological conditions [4]. MFAP2, also known as microfibril-associated glycoprotein 1 (MAGP1), is a small glycoprotein located in microfibrils [5]. Previous studies have indicated that MFAP2 is involved in vascular development and metabolic disease [6]. Recent studies have indicated that MFAP2 plays a significant role in the progression of several tumors and thus might lead to the development of potential biomarkers or novel therapies for cancers [7,8]. Chen *et al.* [9] reported that melanoma cell migration and invasion are inhibited by downregulating MFAP2 through regulation of the Wnt/β-catenin signaling pathway and epithelial-mesenchymal transition (EMT). Wang *et al.* [10] suggested that MFAP2 promotes EMT in gastric cancer (GC) via the

transforming growth factor beta (TGF-β)/SMAD family member 2 (SMAD2)/SMAD3 signaling pathway. Currently, the role and function of MFAP2 in OSCC are incompletely understood.

Autophagy plays a significant regulatory role in tumorigenesis and is closely related to the occurrence and development of tumors. In addition, the level and function of autophagy vary in different cancers [11]. Therefore, autophagy promotes either cell survival or cell death, and the regulation of autophagy is critical for tumorigenesis and tumor development. Currently, the involvement of MFAP2 in the autophagic development of OSCC is unknown. The conserved Wnt signaling pathway is one of the core pathways regulating tissue development and homeostasis [12]. Moreover, the classical Wnt/β-catenin signaling pathway has a vital function in the development of various tumors [13]. Furthermore, β-catenin can regulate tumor epithelia and the tumor microenvironment, making it an attractive therapeutic target in OSCC [14]. Recent studies have indicated the presence of crosstalk between the Wnt/β-catenin signaling pathway and autophagy in different stages of cancer [15,16]. Abnormal Wnt signaling and autophagy disruption contribute to the development and progression of various cancers [17]. Chen *et al.* [18] observed that downregulation of Wnt/β-catenin signaling inhibits autophagy, subsequently inhibiting osteogenic differentiation, and that induction of autophagy positively regulates Wnt/β-catenin signaling. Turcios *et al.* [19] revealed that disruption of autophagic flux inhibits Wnt/β-catenin signaling, thereby suppressing hepatocellular carcinoma. However, the relationship between autophagy, Wnt/β-catenin, and MFAP2 in OSCC remains unclear.

Materials and Methods

Acquisition of data

MFAP2 gene expression data in 33 kinds of cancers were downloaded from The Cancer Genome Atlas (TCGA) database. Based on the data, R language (version 4.2.1) was used to carry out pan-cancer and survival analyses. OSCC accounts for approximately 90% of head and neck squamous cell carcinoma (HNSCC) [20]; therefore, the bioinformatics data for HNSCC were used to represent OSCC data in this study.

Eighteen tissue samples from patients with OSCC and six paracancerous tissues were provided by the Tianjin First Central Hospital (Tianjin, China). The ethics committee of Tianjin Medical University approved the collection and use of clinical samples (Approval No. TMUhMEC20220818), which were carried out following the tenets of the 1964 Declaration of Helsinki. Signed informed consent was received from each patient.

Cell culture

SCC15, SCC25, and CAL27 cells were obtained from Procell Life Science & Technology Co, Ltd. (Wuhan, China). High glucose Dulbecco's Modified Eagle's medium (DMEM) supplemented with 10% fetal bovine serum (FBS) and 1% penicillin/streptomycin (Procell Life Science &Technology Co, Ltd.) was used to culture the cells at 37°C in a humidified incubator under 5% CO_2.

Cell transfection

For knockdown of *MFAP2*, a small interfering (si)RNA targeting *MFAP2* (si-MFAP2, 5′-CCAUACACAGGCCUUGCAATT-3′ and 5′-UUGCAAGGCCUGUGUAUGGTT-3′) and the corresponding negative control (NC, 5′-UUCUCCGAACGUGUCACGUTT-3′ and 5′-ACGUGACACGUUCGGAGAATT-3′) were designed by Suzhou Genepharma Co. Ltd (Suzhou, China). For *MFAP2* overexpression, *MFAP2* overexpression plasmid (pcDNA3.1(+), oeMFAP2) and control vector were also purchased from Suzhou Genepharma Co. Ltd, Suzhou, China.

One day before transfection, SCC15 cells (2×10^5 cells/well) were seeded in 6-well plates and cultured to 50%–70% confluence. Subsequently, siRNAs targeting *MFAP2* or an *MFAP2* overexpression plasmid was transfected into the cells separately using si-RNAMate (Suzhou Genepharma Co. Ltd) following the manufacturer's protocol, with incubation at 37°C in a humidified incubator under 5% CO_2. At 6 h after transfection, DMEM was used to replace the transfection mixture. At 24 h after transfection, the transfected cells could be employed in experiments.

Cell counting kit-8 (CCK8) assay

SCC15 cells (2×10^3 cells/mL) were added to the wells of 96-well plates and incubated for 24 h before transfection. At 24 h after transfection, 10 μL CCK8 reagent (Biosharp Life Science, Hefei, China) was added to each well and incubated at 37°C for 1 h. The viability of SCC15 cells in each well was detected by measuring the absorbance at 450 nm. The results were analyzed using GraphPad software (GraphPad Software, Inc., San Diego, USA).

Colony formation assay

Colony formation assay was performed to investigate cell proliferation. SCC15 cells (1000 cells) were seeded in a 60 × 15 mm dish with DMEM (5 mL) after preparing single cell suspensions. Cells were cultured for 14 days, followed by two times wash with phosphate-buffered saline (PBS), and then fixed using 4% paraformaldehyde at room temperature for 20 min. After two times wash with PBS, the cells were stained with 0.1% hematoxylin for 30 min. After two further washes with PBS, the colonies were photographed with a digital camera and counted.

Flow cytometry analysis

SCC15 cells were digested using EDTA-free trypsin (Beyotime, Nantong, China) at 24 h after transfection. Then, 5×10^5 cells were resuspended in 1 × Annexin binding buffer (1 mL), and 100 μL of the cell suspension was added to a 1.5 mL conical tube containing 5 μL of fluorescein isothiocyanate (FITC) Annexin V and 5 μL of propidium iodide (PI). The suspension was mixed gently and placed in the dark for 10 min at room temperature. A BD Pharmingen™ FITC Annexin-V apoptosis detection kit (BD Biosciences, San Jose, USA) was then used to detect apoptosis. A FACSCalibur flow cytometer (BD Biosciences) was used to analyze the binding of FITC Annexin V and PI to the cells using Cell Quest software.

Wound healing and Transwell assays

SCC15 cells (2×10^5 cells/mL) were added to the wells of a 6-well plate and grown for 24 h until the cells showed confluent growth. The confluent cell layer was then scratched using a 200-μL pipette tip. The wound was photographed under a microscope after the scratch was made and after 24 h and 48 h of incubation in serum-free medium (2 mL/well) at 37°C to calculate wound healing.

At 24 h after transfection, SCC15 cells (1×10^5 cells/mL) in 200 μL of serum-free DMEM were placed in the upper chamber of a Transwell apparatus. Then, 600 μL of complete medium was added to the lower chamber. The Transwell chambers were incubated for

48 h, after which the non-migrated cells were carefully removed, and the invaded cells were fixed using 4% formaldehyde for 10 min, followed by staining with 0.1% hematoxylin for 30 min. The invaded cells were photographed under a microscope at 48 h. Leica Application Suite X (LAS X) software (Leica, Wetzlar, Germany) was used to process the images, and ImageJ (NIH, Bethesda, USA) was used to carry out the quantitative analysis.

Immunohistochemistry (IHC)

Previously prepared sections were subjected to xylene dewaxing and ethanol rehydration, washed with PBS, and then blocked with 5% bovine serum albumin (BSA) at room temperature for 30 min. After washing, primary antibodies against MFAP2 (1:450, ab231344; Abcam, Cambridge, UK) were added to the sections and incubated overnight at 4°C. The next day, the sections were stained using a Universal two-step assay kit (mouse/rabbit reinforced polymer assay system; Zhong Shan Jin Qiao, Beijing, China). Images were processed using Leica Application Suite X (LAS X) software.

Immunofluorescence assay

At 48 h after transfection, the SCC15 cells were blocked with goat serum for 2 h at room temperature, incubated in primary antibody (anti-LC3B monoclonal antibodies, 1:200, ET1701-65; Huabio, Hangzhou, China) overnight at 4°C, and then with FITC-conjugated secondary antibody (dilution: 1:1000; Beyotime Institute of Biotechnology, Shanghai, China) for 1 h at room temperature. Subsequently, 4′,6-diamidino-2-phenylindole (DAPI; Beyotime) was utilized to label the nuclei. Immunofluorescence images were acquired by confocal microscopy and Zen software (Carl Zeiss, Oberkochen, Germany). Quantitative analysis was performed using ImageJ software.

Transmission electron microscopy

At 48 h after transfection, the culture medium was discarded, and the SCC15 cells were fixed with electron microscope fixing solution (G1102; Wuhan Google Biotechnology, Wuhan, China) for 2–4 h and then wrapped in 1% agarose. After washing with 0.1 M phosphate buffer (PB, pH 7.4), the cells were fixed with 1% osmium for 2 h at room temperature. The cells were dehydrated with graded acetone, permeated with epoxy resin, embedded, sectioned, and stained with uranyl acetate and lead citrate. The sections were examined using an HT770 transmission electron microscope (Hitachi, Tokyo, Japan) at an accelerating voltage of 80 kV to observe autophagosomes and autolysosomes.

Quantitative real-time reverse transcription polymerase chain reaction (qRT-PCR)

The TRIzol reagent (Life Technologies, Carlsbad, USA) was used to extract cellular RNA, which was then reverse-transcribed into cDNA using a reverse transcription kit (Takara, Shiga, Japan). The quantitative real-time PCR (qPCR) was performed on a CFX96™ Optics Module system using iQ™ SYBR® Green Supermix (Bio-Rad, Hercules, USA). Primers were designed using the National Center for Biotechnology Information (NCBI) Primer Blast. The sequences are as follows: *MFAP2* Forward 5′-TCTTCCTGCTATTCCTGCCTG-3′, Reverse 5′-AGTCTGGGTTGTCGATCTGG-3′; *ATCB* Forward 5′-TCA CCATGGATGATGATATCGC-3′, Reverse 5′-ATAGGAATCCTTCT GACCCATGC-3′. The mRNA expressions were calculated using the $2^{-\Delta\Delta CT}$ method. The expression of the housekeeping gene *ATCB* (encoding β-actin) was detected as the reference control.

Western blot analysis

Total proteins in SCC15 cells at 48 h after transfection and animal tissues were lysed on ice using radioimmunoprecipitation assay lysis buffer (Solarbio, Beijing, China), followed by centrifugation at 13,800 *g* at 4°C for 10 min to obtain total proteins. The protein concentration in the supernatant was determined using a BCA protein assay kit (Solarbio). Next, loading buffer (Biosharp Life Science) was added to the protein sample and boiled for 10 min to denature and depolymerize the proteins. Sodium dodecyl sulfate polyacrylamide gel electrophoresis was applied to separate equal amounts of protein samples on 4%–12% pre-cast gradient gels (M41212C; GenScript, Piscataway, USA) before being transferred electrophoretically onto an immobilon-P transfer membrane (Merck Millipore Ltd., Carrigtwohill, Ireland). After block for 2 h at room temperature using 5% non-fat milk, the membranes were incubated with primary antibodies at 4°C overnight. The primary antibodies are as follows: anti-MFAP2 polyclonal antibody (1:1000; Abcam), anti-Bax polyclonal antibody (1:1000; Cell Signaling Technology, Danvers, USA), anti-Bcl-2 polyclonal antibody (1:1000; Wuhan Sanying Biotechnology, Wuhan, China), anti-LC3B monoclonal antibody (1:1000; Huabio, Hangzhou, China), anti-P62 monoclonal antibody (1:1000; Abcam), anti-Beclin 1 monoclonal antibody (1:1000; Abcam), anti-Atg5 monoclonal antibody (1:1000; Abcam), anti-Atg7 monoclonal antibody (1:1000; Abcam), anti-β-catenin polyclonal antibody (1:2000; Wuhan Sanying Biotechnology), anti-MMP9 monoclonal antibody (1:1000; Abcam), anti-c-Myc polyclonal antibody (1:1000; Wuhan Sanying Biotechnology), anti-Cyclin D1 antibody (1:2000; Wuhan Sanying Biotechnology), anti-Survivin monoclonal antibody (1:1000; Cell Signaling Technology), anti-Lamin B1 polyclonal antibody (1:1000; Wuhan Sanying Biotechnology), and anti-GAPDH polyclonal antibody (1:10,000; Bioworld, Minneapolis, USA). The next day, the membranes were further incubated with secondary antibodies comprising goat anti-rabbit IgG (H + L) (1:10,000; Bioworld) at room temperature for 1 h. An Amersham imager 680 (GE, Boston, USA) was used to visualize the immunoreactive protein bands. Quantitative analysis was performed using ImageJ software.

Animal experiments

Four-week-old female BALB/C nude mice (Beijing Weitong Lihua Biotechnology Co., Ltd, Beijing, China) were randomly divided into three groups and treated with *MFAP2*-knockdown cells (stably transfected with sh-MFAP2 lentiviral transduction particles), negative control cells (stably transfected with sh-NC lentiviral transduction particles) (Shanghai Jikai Gene Chemical Technology Co., Ltd, Shanghai, China), or untreated control cells. A total of 1×10^6 cells suspended in 200 μL PBS were then injected into the right subaxillary region of the mice. The size of the tumors was measured with digital callipers every three days, and the tumor volume (length × width^2/2) was calculated. The animal experiments were approved by the Experimental Animal Ethics Committee of Tianjin Institute of Environmental and Operational Medicine (Approval No: 04-2022-041).

Statistical analysis

All statistical analyses were carried out using SPSS statistics version

25.0 (IBM Corp., Armonk, USA). The Shapiro-Wilk normality test was used to test the normality of the data. For two-group comparisons, Student's *t*-test was adopted, while for comparisons of more than two groups, one-way ANOVA was used. The statistical significance threshold was set at $P < 0.05$.

Results

The expression and prognostic value of MFAP2 in OSCC

The TCGA database was used to investigate the differential transcription of *MFAP2* in various cancers and in normal tissues. *MFAP2* expression was markedly upregulated in several cancers (Figure 1A). To determine *MFAP2* expression in OSCC, data for patients with HNSCC from the TCGA database were acquired, and a volcano plot was generated, which showed that *MFAP2* expression was upregulated in HNSCC (Figure 1B). Higher MFAP2 expression was detected in HNSCC compared with that in normal tissue ($P < 0.05$, Figure 1C). To further verify MFAP2 expression in OSCC, the protein expression of MFAP2 was detected by IHC in 6 para-cancerous tissues and 18 OSCC samples. The IHC images revealed that MFAP2 protein expression was low in para-cancerous tissues but high in OSCC tissues (Figure 1D). To determine the impact of *MFAP2* expression on the prognosis of patients with OSCC, the TCGA database was used. This analysis revealed that higher *MFAP2* expression was significantly associated with lower overall survival ($P < 0.05$, Figure 1E). Subsequently, qRT–PCR and western blot analysis were used to detect the mRNA and protein expression levels of MFAP2 in OSCC cell lines (SCC15, SCC25, and CAL27). SCC15 cells exhibited relatively higher MFAP2 mRNA and protein expression levels (Figure 1F,G).

Effects of MFAP2 expression on the viability, proliferation, apoptosis, migration and invasion of OSCC

To explore the biological function of MFAP2 in OSCC, *MFAP2* was knocked down or overexpressed in SCC15 cells. First, the transfection efficiency of si-MFAP2 and oe-MFAP2 was verified using western blotting and qRT-PCR (Figure 2A and Supplementary Figure S1). To explore the effect of MFAP2 on SCC15 cell viability and proliferation, CCK8 and colony formation assays were performed. The results showed a significant reduction in the viability and proliferation of SCC15 cells after *MFAP2* knockdown

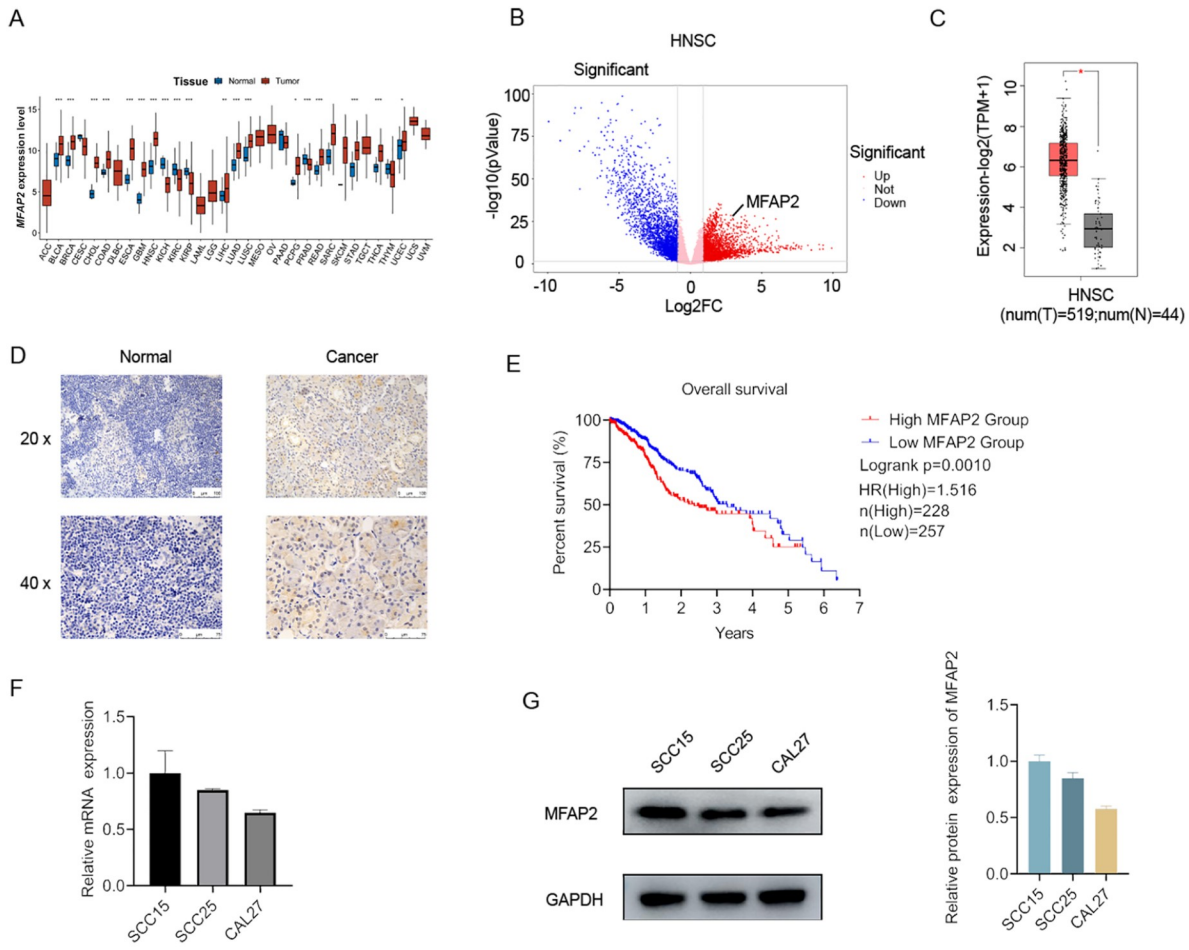

Figure 1. MFAP2 expression is upregulated in OSCC and correlates with poor prognosis of patients with OSCC (A) The mRNA expression levels of *MFAP2* in multiple cancers. (B) A volcano plot showing high expression of *MFAP2* in HNSCC ($n = 566$, $P < 0.05$). (C) A box plot showing the mRNA expression levels of *MFAP2* in HNSCC. HNSCC samples are outlined in red, while normal samples are outlined in black. Data are presented as the mean ± standard deviation $^*P < 0.05$. (D) Immunohistochemistry images showing high levels of MFAP2 in OSCC tissues ($n = 18$, $P < 0.05$). (E) The overall survival curve plot of patients with HNSCC with low and high mRNA expression of *MFAP2* (TCGA database). (F) *MFAP2* mRNA expression in three OSCC lines. (G) The protein level of MFAP2 in three OSCC lines. The band intensity was quantified using ImageJ ($n = 3$ per group).

via si-RNA. To further assess MFAP2's influence on SCC15 cell viability and proliferation, the cells were transfected with the *MFAP2* overexpression plasmid. *MFAP2* overexpression had the opposite results to those of the si-MFAP2 group. Thus, MFAP2 has a positive role in regulating OSCC cell viability and proliferation (Figure 2B,C). Subsequently, flow cytometry was used to assess the effect of MFAP2 on SCC15 cell apoptosis. The apoptosis rate increased significantly in the si-MFAP2 group, while overexpression of *MFAP2* did not affect the apoptosis rate in SCC15 cells. These results confirmed that knockdown of *MFAP2* promotes apoptosis in OSCC (Figure 2D). Additionally, the effects of *MFAP2* knockdown and overexpression on SCC15 cell migration and invasion were further assessed using wound healing and Transwell assays, respectively. Compared with that in the control and si-NC groups, the migration rate of SCC15 cells in the si-MFAP2 group was significantly decreased ($P < 0.05$, Figure 2E). The oe-MFAP2 group showed increased migratory capability compared with the control and oe-NC groups ($P < 0.05$). Compared with that in the control and si-NC groups, the invasion rate of the SCC15 cells in the si-MFAP2 group was significantly decreased ($P < 0.05$). The oe-MFAP2 group showed increased invasive capability compared with the control and oe-NC groups ($P < 0.05$, Figure 2F). Based on these results, the high expression of MFAP2 might enhance the migrative and invasive abilities of OSCC.

MFAP2's impact on OSCC biological behavior by regulating autophagy

The occurrence and development of tumors are closely associated with autophagy. To explore whether autophagy is involved in the effect of MFAP2 on SCC15 cells, western blotting was used to determine the effects of *MFAP2* silencing and overexpression on the levels of autophagy-related proteins. After downregulating *MFAP2* expression, the protein levels of Atg7, Atg5, LC3B, and Beclin-1 were significantly decreased, while the protein level of P62 was significantly increased compared with those in the control and si-NC groups. In the oe-MFAP2 group, the protein levels of Atg7, Atg5, LC3B, and Beclin-1 were significantly increased, while the protein level of P62 was significantly decreased compared with those in the control and oe-NC groups. In addition, to clarify the underlying mechanism of MFAP2-induced cell apoptosis, the levels of apoptosis-related proteins (Bax and Bcl-2) were detected using western blotting. Bax was upregulated, while Bcl-2 was downregulated, in the si-MFAP2 group compared with that in the control and si-NC groups. The opposite results were obtained after overexpressing *MFAP2* in SCC15 cells (Figure 3A). In addition, immunofluorescence revealed that LC3B immunofluorescence intensity was significantly decreased in the si-MFAP2 group compared with the control and si-NC groups. LC3B immunofluorescence intensity was significantly increased in the oe-MFAP2 group compared with the control and oe-NC groups ($P < 0.05$, Figure 3B). In the later stage of autophagy, autophagosomes and lysosomes form autolysosomes, where autophagosomal-sequestered cargo is degraded by lysosomes. The autophagosomes observed by electron microscopy were very limited, while some autolysosomes were observed. The autolysosomes could represent the autophagic level; therefore, we marked autolysosomes. The number of autolysosomes was decreased in the si-MFAP2 group compared with the control and si-NC groups (Figure 3C). The number of autolysosomes was increased in the oe-MFAP2 group compared with the control and oe-NC groups (Figure 3D).

To further explore the correlation between MFAP2 and autophagy, SCC15 cells were cultured with rapamycin (100 nM/mL; MCE, Monmouth junction, USA). The viability and proliferation of SCC15 cells were significantly increased in the si-MFAP2 group after treatment with rapamycin, as detected by CCK8 and colony formation assays (Figure 4A,B). In addition, SCC15 cell apoptosis decreased significantly in the siMFAP2 + rapamycin group compared with that in the si-MFAP2 group, as assessed by flow cytometry (Figure 4C). Moreover, the migration (wound healing) and invasion (Transwell assays) abilities of *MFAP2*-knockdown

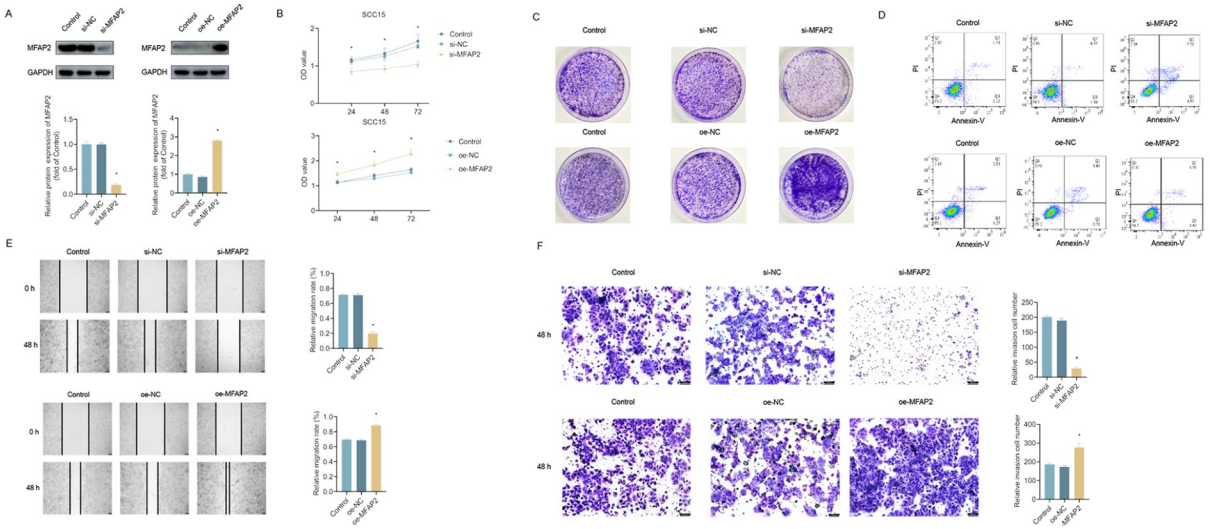

Figure 2. Effects of MFAP2 expression on SCC15 cell viability, proliferation, apoptosis, migration, and invasion (A) Efficiency of *MFAP2* knockdown and overexpression in SCC15 cells, as confirmed western blotlting. The band intensity was quantified using ImageJ ($n = 3$ per group) $^*P < 0.05$ compared with the control. (B) Viability of SCC15 cells with *MFAP2* knockdown or overexpression ($n = 3$ per group), $^*P < 0.05$ compared with the control. (C) Proliferation of SCC15 cells with *MFAP2* knockdown or overexpression. (D) Apoptosis of SCC15 cells with *MFAP2* knockdown or overexpression. (E) Migration of SCC15 cells with *MFAP2* knockdown or overexpression ($n = 10$ per group), $^*P < 0.05$ compared with the control. (F) Invasion of SCC15 cells with *MFAP2* knockdown or overexpression (n = 10 per group). $^*P < 0.05$ compared with the control.

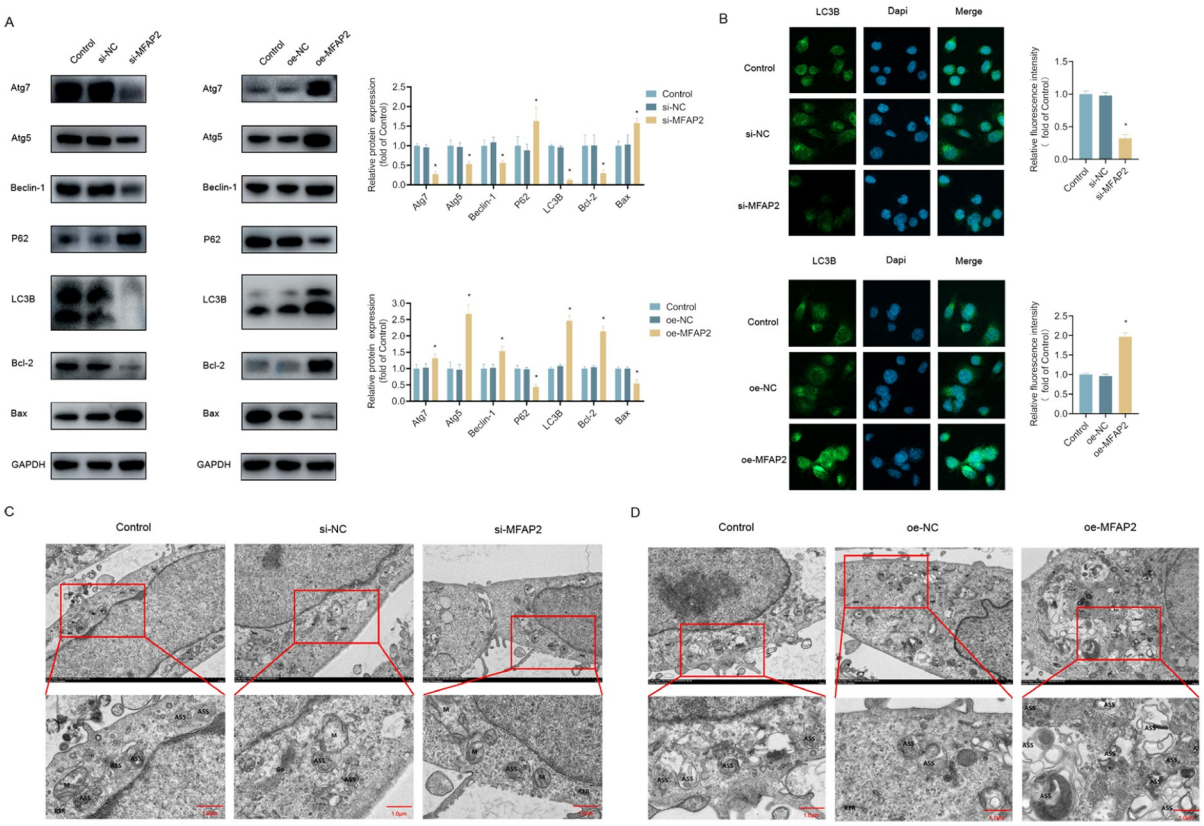

Figure 3. The effect of MFAP2 on autophagy (A) The autophagy- and apoptosis-related protein levels in SCC15 cells with knockdown or overexpression of *MFAP2*. The band intensity was quantified using ImageJ ($n=3$ per group), $^*P<0.05$ compared with the control. (B) Representative LC3B immunofluorescence staining and LC3B intensity ($n=6$ per group), $^*P<0.05$ compared with the control. (C,D) Representative autolysosomes in SCC15 cells with knockdown or overexpression of *MFAP2* (N: Nucleus; Nu: Nucleolus; M: Mitochondria; RER: Rough endoplasmic reticulum; ASS: Autolysosome; AP: Autophagosome; LP: Lipid droplet; GO: Golgi).

SCC15 cells were increased after treatment with rapamycin (Figure 4D,E).

The potential mechanism of this phenomenon was further explored by determining the levels of autophagy- and apoptotic pathway-related proteins using western blotting. The protein levels of Atg7, Atg5, LC3B, and Beclin-1 increased significantly, while that of P62 decreased significantly in the si-MFAP2 + Rapamycin group compared with those in the si-MFAP2 group. In parallel, Bax protein levels decreased significantly, while Bcl-2 levels increased significantly in the si-MFAP2 + Rapamycin group compared with the si-MFAP2 group (Figure 4F). In summary, Rapamycin can activate autophagy and reverse the effect of si-MFAP2 on SCC15 cells. Thus, we inferred that MFAP2 can affect the biological behavior of OSCC by regulating autophagy. In addition, recent studies have reported that autophagy has a vital function during cancer development and interacts with components of the Wnt/β-catenin signaling pathway [21,22]. We first determined the levels of Wnt/β-catenin signaling pathway-related proteins after transfection with si-MFAP2. The results indicated that β-catenin, MMP9, c-Myc, Cyclin D1, and Survivin levels were significantly downregulated after *MFAP2* silencing in SCC15 cells. Silencing *MFAP2* could inhibit autophagy in OSCC; therefore, we inferred that inhibition of autophagy might suppress Wnt/β-catenin signaling. After treatment with rapamycin, the β-catenin, MMP9, c-Myc, Cyclin D1, and Survivin levels were significantly upregulated in *MFAP2*-silenced SCC15 cells. The results indicated that in OSCC, the activation of autophagy might upregulate β-catenin levels and its downstream molecules in the Wnt/β-catenin signaling pathway (Figure 4G).

MFAP2 affects the biological behavior of OSCC cells via Wnt/β-catenin signaling pathway regulation

To further determine whether MFAP2 affects Wnt/β-catenin signaling, we performed western blotting analysis. The level of β-catenin, a core factor in Wnt/β-catenin signaling, was significantly downregulated in *MFAP2*-knockdown cells. Furthermore, the protein levels of downstream molecules of β-catenin, including MMP9, c-Myc, Cyclin D1, and Survivin, were significantly downregulated in the si-MFAP2 group compared with those in the control and si-NC groups. In contrast, *MFAP2* overexpression increased β-catenin level, which suggested that MFAP2 might regulate β-catenin expression at the transcriptional level. The protein levels of MMP9, c-Myc, Cyclin D1, and Survivin were significantly upregulated in *MFAP2*-overexpressing cells (Figure 5A).

To further explore the correlation between MFAP2 and the Wnt/β-catenin signaling pathway, SCC15 cells were cultured with a GSK3β inhibitor (6 μM/mL, CHIR99021; Selleck, Houston, USA). CCK8 and colony formation assays demonstrated that CHIR99021 significantly increased SCC15 cell in the si-MFAP2 + CHIR99021 group compared with the si-MFAP2 group (Figure 5B,C). Subsequent flow cytometry analysis showed that CHIR99021 significantly decreased the apoptosis of SCC15 cells in the si-MFAP2 + CHIR99021 group compared with that in the si-MFAP2 group

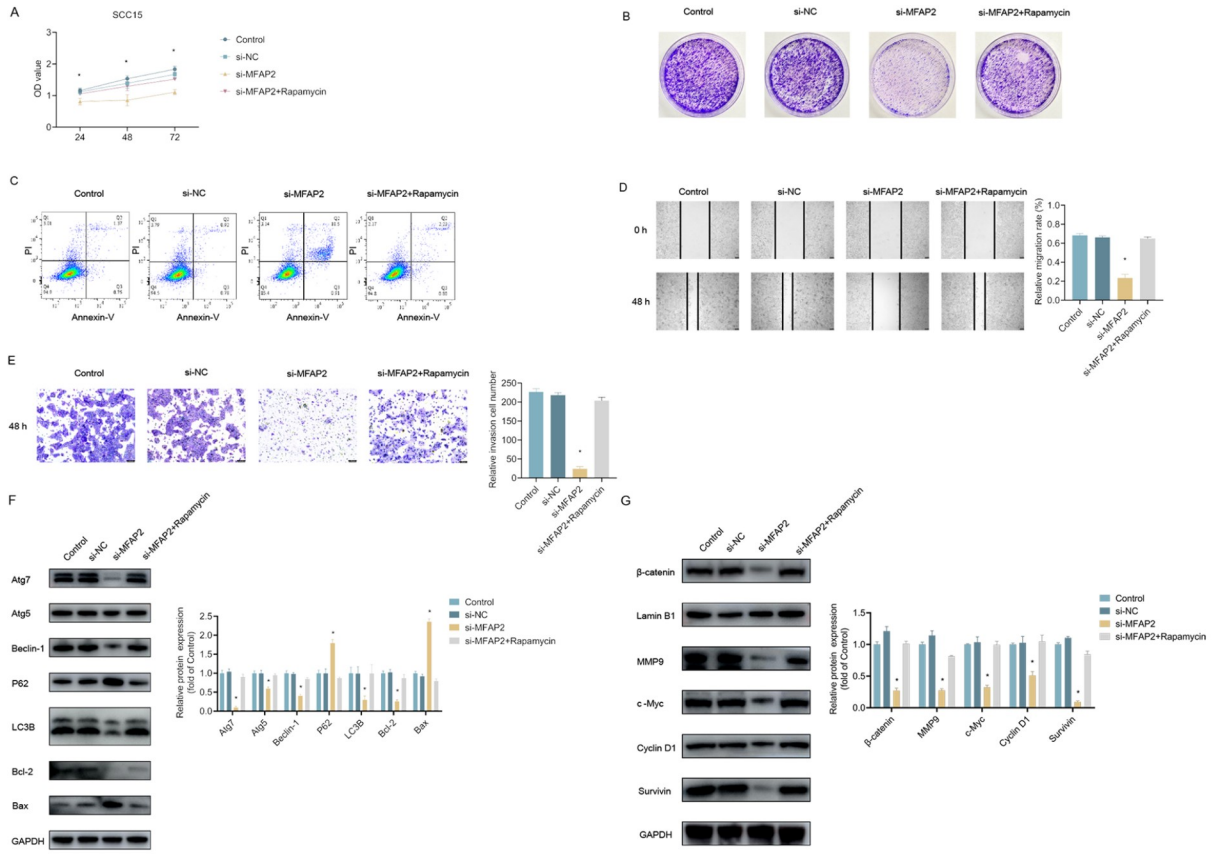

Figure 4. MFAP2's impact on the viability, proliferation, apoptosis, migration, and invasion of OSCC by inhibiting autophagy (A) Viability of SCC15 cells after *MFAP2* knockdown and adding rapamycin ($n = 3$ per group), $^*P < 0.05$ compared with the control. (B) Proliferation of SCC15 cells after *MFAP2* knockdown and the addition of rapamycin. (C) Apoptosis of SCC15 cells after *MFAP2* knockdown and the addition of rapamycin. (D) Migration of SCC15 cells after MFAP2 knockdown and the addition of rapamycin ($n = 10$ per group), $^*P < 0.05$ compared with the control. (E) Invasion of SCC15 cells after *MFAP2* knockdown and the addition of rapamycin ($n = 10$ per group), $^*P < 0.05$ compared with the control. (F) The autophagy-related protein levels in SCC15 cells after *MFAP2* knockdown and the addition of rapamycin. The band intensity was quantified using ImageJ ($n = 3$ per group), $^*P < 0.05$ compared with the control. (G) The protein levels of β-catenin and its related downstream proteins in SCC15 cells after *MFAP2* knockdown and rapamycin treatment. The band intensity was quantified using ImageJ ($n = 3$ per group), $^*P < 0.05$ compared with the control.

(Figure 5D). Moreover, the migratory and invasive abilities of *MFAP2*-knockdown SCC15 cells were increased by CHIR99021 via Wnt/β-catenin signaling activation. These results suggested that migratory and invasive abilities of *MFAP2*-knockdown SCC15 cells were increased after treatment with CHIR99021 (Figure 5E,F).

To further probe the mechanism of this increase, the levels of Wnt/β-catenin signaling and apoptotic pathway-related proteins were assessed by western blotting. The results showed that the levels of β-catenin, MMP9, c-Myc, Cyclin D1, and Survivin were significantly upregulated in the si-MFAP2 + CHIR99021 group compared with those in the si-MFAP2 group. Furthermore, Bax level were significantly downregulated, while Bcl-2 levels were significantly upregulated, in *MFAP2*-knockdown SCC15 cells treated with CHIR99021 (Figure 5G). Taken together, CHIR99021 activates Wnt/β-catenin signaling and reverses the effect of si-MFAP2 on SCC15 cells. Therefore, MFAP2 expression is involved in the progression of OSCC in a Wnt/β-catenin-dependent manner. To detect whether the Wnt/β-catenin pathway can regulate autophagy, the protein levels of autophagy-related factors in SCC15 cells treated with CHIR99021 were assessed using western blotting. After treatment with CHIR99021, the Atg7, Atg5, Beclin-1, P62, and LC3B levels did not show significant changes compared with the si-MFAP2 group. The results further indicated that MFAP2 could regulate the Wnt/β-catenin signaling pathway through autophagy (Figure 5H).

Downregulated MFAP2 inhibits tumor growth in OSCC *in vivo*

The xenograft tumor model was established to explore the effects of MFAP2 protein expression level on tumor growth of OSCC *in vivo*. Compared with that in the control and sh-NC groups, the tumor volume in the sh-MFAP2 group was significantly decreased ($P < 0.05$; Figure 6A–C). The tumor weight in the sh-MFAP2 group was significantly decreased compared with that in the control and sh-NC groups ($P < 0.05$; Figure 6D). Western blotting results indicated that the protein levels of Atg7, Atg5, LC3B, Beclin-1, β-catenin, c-Myc, and Cyclin D1 were significantly downregulated in the sh-MFAP2 group compared with the control and sh-NC groups (Figure 6E), which was consistent with the *in vitro* results.

Discussion

Research indicates that MFAP2 is associated with several cancers,

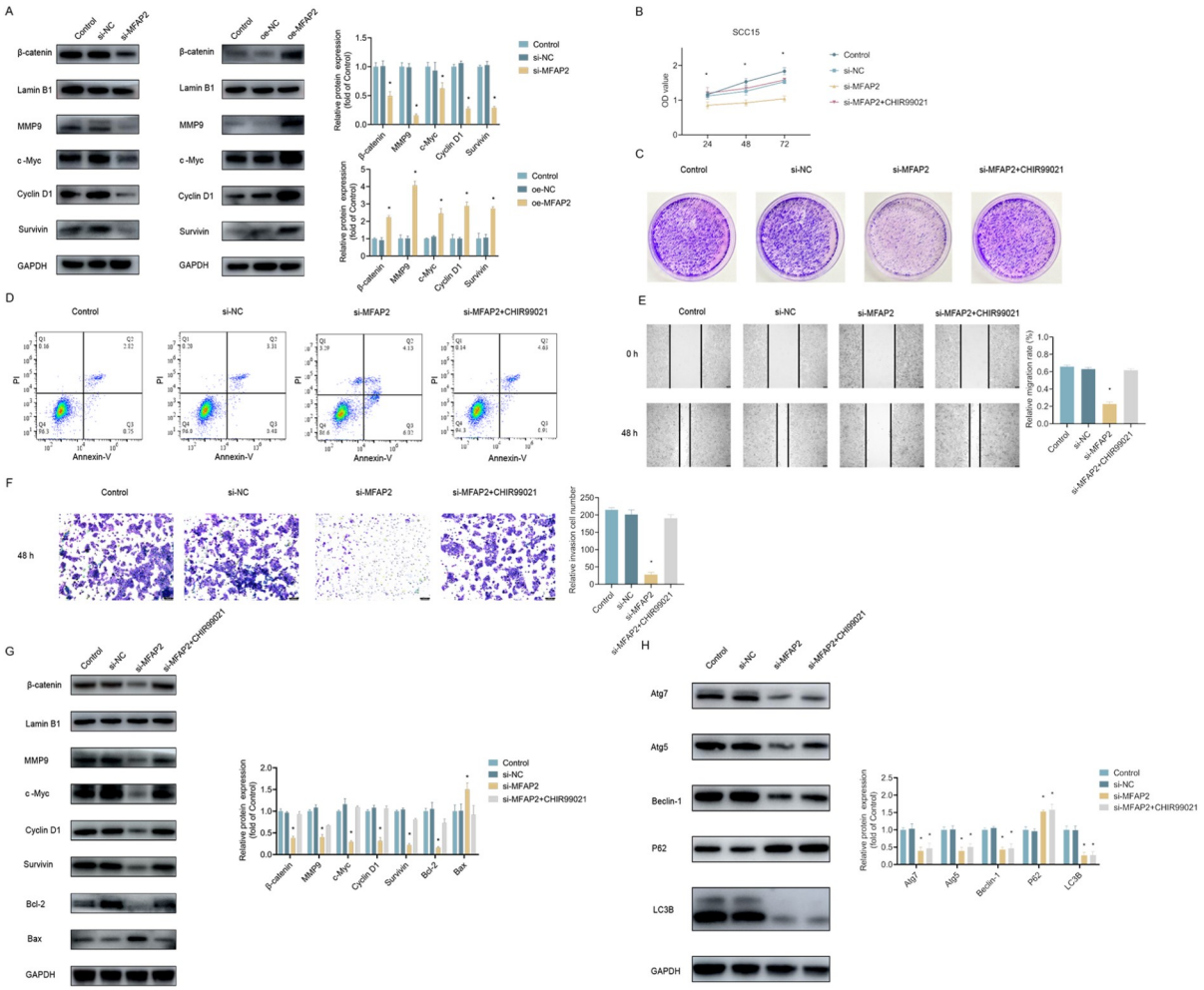

Figure 5. MFAP2's impact on viability, proliferation, apoptosis, migration, and invasion of OSCC via regulation of Wnt/β-catenin signaling (A) The β-catenin and relevant downstream protein levels in SCC15 cells after knockdown or overexpression of *MFAP2*. The band intensity was quantified using ImageJ ($n=3$ per group), $^*P<0.05$ compared with the control. (B) Viability of SCC15 cells after *MFAP2* knockdown and the addition of CHIR99021 ($n=3$ per group), $^*P<0.05$ compared with the control. (C) Proliferation of SCC15 cells after *MFAP2* knockdown and the addition of CHIR99021. (D) Apoptosis of SCC15 cells after *MFAP2* knockdown and the addition of CHIR99021. (E) Migration of SCC15 cells after MFAP2 knockdown and addition of CHIR99021 ($n=10$ per group), $^*P<0.05$ compared with the control. (F) Invasion of SCC15 cells after MFAP2 knockdown and the addition of CHIR99021 ($n=10$ per group), $^*P<0.05$ compared with the control. (G) The β-catenin and relevant downstream protein levels in SCC15 cells after MFAP2 knockdown and addition of CHIR99021. The band intensity was quantified using ImageJ ($n=3$ per group), $^*P<0.05$ compared with Control. (H) The autophagy-related protein levels in SCC15 cells after *MFAP2* knockdown and the addition of CHIR99021. The band intensity was quantified using ImageJ ($n=3$ per group), $^*P<0.05$ compared with the control.

suggesting that MFAP2 could be an important prognostic biomarker and target for cancer immunotherapy [7]. Segura *et al.* [23] suggested that MFAP2 expression is downregulated in patients with colon cancer and obesity and could be involved in changes in ECM remodeling, resulting in the development of obesity-associated colon cancer. Sun *et al.* [24] performed bioinformatics analysis and revealed that MFAP2 could be a novel diagnostic and prognostic biomarker in patients with GC. Yao *et al.* [25] reported MFAP2 overexpression in GC and noted that downregulation of MFAP2 could inhibit the motility of GC via the MFAP2/integrin α5β1/focal adhesion kinase (FAK)/extracellular regulated protein kinase (ERK) pathway. However, there has been little research on MFAP2 in OSCC. To determine whether there is a biological relationship between MFAP2 and OSCC progression, we used bioinformatics analysis followed by experimental verification in this study. We detected high MFAP2 mRNA and protein expression in OSCC, which might be associated with OSCC development. In addition, knockdown of *MFAP2* inhibited proliferation, migration, and invasion and promoted apoptosis in SCC15 cells, while *MFAP2* overexpression had the opposite effect. Furthermore, there were significant differences in OS between the low- and high-*MFAP2* expression groups, which indicated that high *MFAP2* expression would have a significant effect on OSCC prognosis. In addition, MFAP2 protein downregulation inhibited the xenograft growth of OSCC *in vivo*. These results suggest that MFAP2 exerts a positive regulatory effect on OSCC tumorigenesis and metastasis.

Furthermore, we revealed that MFAP2 positively regulates autophagy in OSCC. Accumulating evidence indicates that autophagy, a mechanism that maintains cellular homeostasis, has a vital function in the formation, development, and treatment of cancers

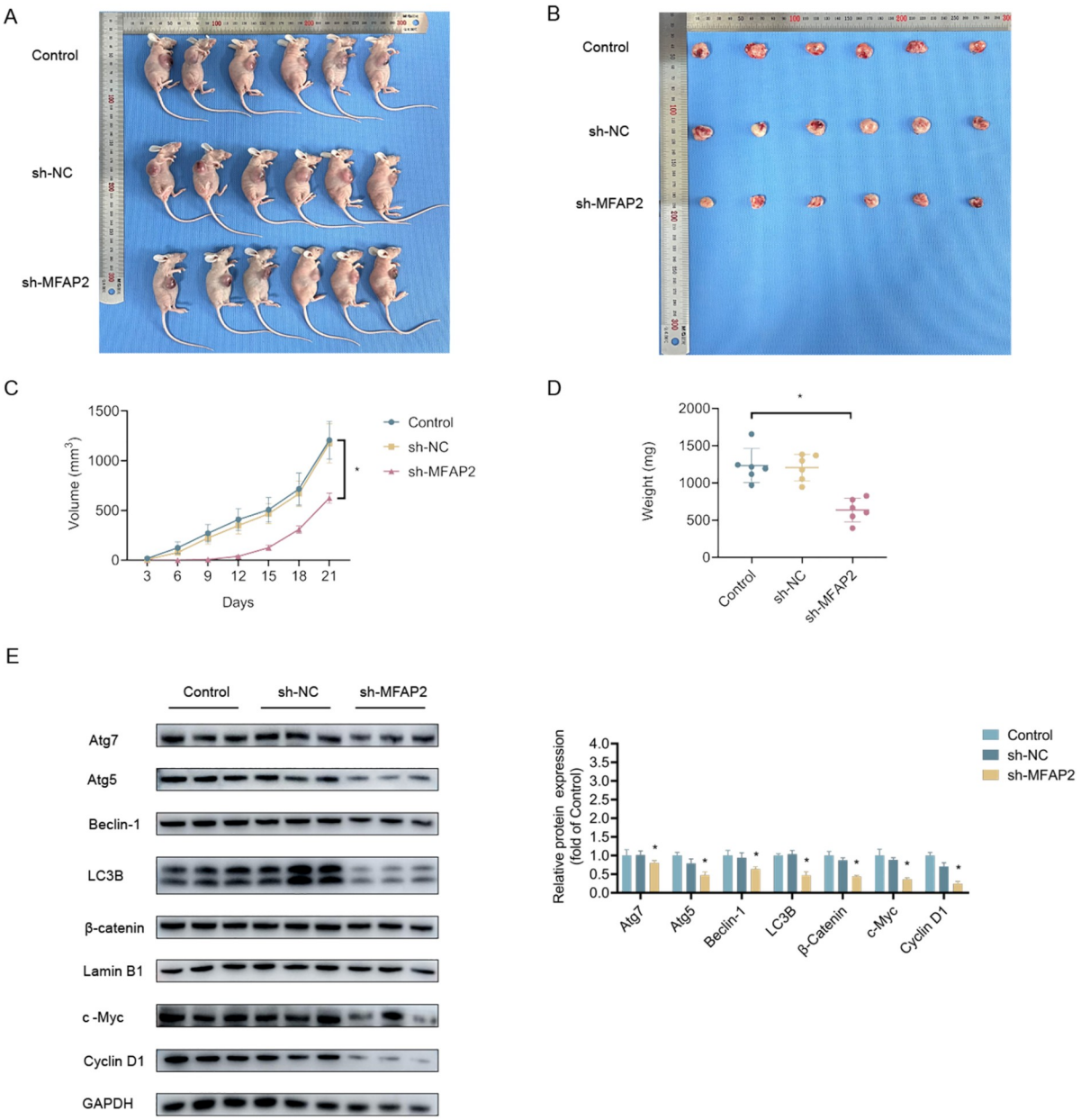

Figure 6. *MFAP2* knockdown inhibits OSCC tumor growth *in vivo* (A,B) Female BALB/C nude mice and xenografts at 21 days after subcutaneous injection. (C,D) Statistical analysis of tumor volume and weight after subcutaneous injection. (E) The protein expression levels of relevant factors of autophagy and the Wnt/β-catenin pathway. The band intensity was quantified using ImageJ ($n = 3$ per group), $^*P < 0.05$ compared with the control.

[26,27]. Marsh *et al.* [28]suggested that genetic autophagy inhibits primary tumor growth and metastasis in breast cancer by regulating the autophagy cargo receptor NBR1. Peng *et al.* [29] argued that circular RNA CUL2 might inhibit the development of gastric cancer and regulate cisplatin sensitivity via autophagy activation through the miR-142-3p/Rho associated coiled-coil containing protein kinase 2 (ROCK2) axis. Moreover, it has been confirmed that autophagy is closely related to OSCC [30]. The results of the present study indicated that *MFAP2* knockdown suppressed autophagy, while overexpression of MFAP2 induced autophagy in SCC15 cells, suggesting an oncogenic role of excessive autophagy in OSCC. To further verify the relationship between MFAP2 and autophagy in SCC15 cells, we carried out rescue assays. The results indicated that rapamycin could activate autophagy and counteract the effect of silencing *MFAP2* in SCC15 cells. Importantly, *MFAP2* knockdown disrupted autophagy in OSCC, suggesting that OSCC progression is regulated via MFAP2-induced autophagy.

Similarly, we discovered that MFAP2 positively regulates Wnt/β-catenin signaling in OSCC. The Wnt/β-catenin signaling pathway has an essential function in cell proliferation and metastasis regulation [31,32]. Abnormal activation of Wnt/β-catenin signaling leads to the occurrence and development of several types of cancers [33,34]. In this study, *MFAP2* knockdown inhibited the Wnt/β-catenin signaling pathway, while *MFAP2* overexpression had the opposite effect. The cells treated with CHIR99021 showed restored malignant biological behavior, which was attenuated by *MFAP2*

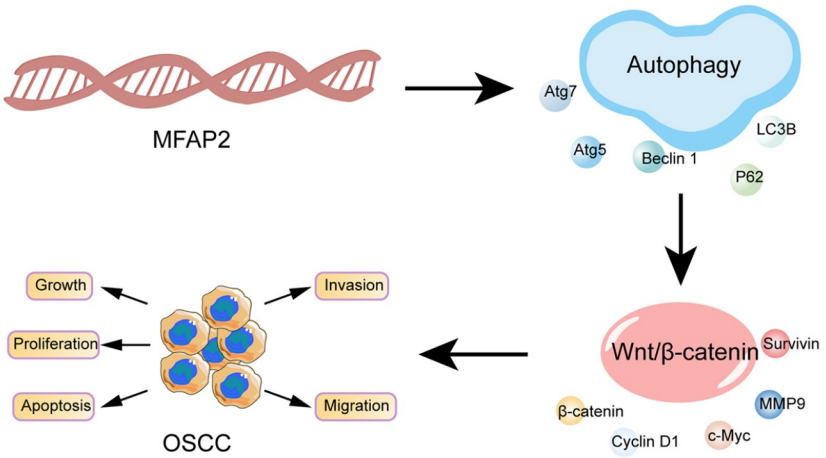

Figure 7. A schematic diagram showing that MFAP2 can influence OSCC progression via its autophagic regulation of Wnt/β-catenin signaling

knockdown. From this, we could infer that MFAP2 regulates tumorigenesis and the development of OSCC in a manner dependent on Wnt/β-catenin signaling. In addition, *MFAP2* knockdown inhibited the protein expressions of relevant factors of autophagy and the Wnt/β-catenin signaling pathway *in vivo*. Taken together, *MFAP2* could regulate autophagy and the Wnt/β-catenin signaling pathway *in vitro*and *in vivo*.

The autophagic mechanism and its crosstalk with Wnt/β-catenin signaling are critical for cellular homeostasis and adaptation to complex environmental conditions. Both autophagy and Wnt/β-catenin signaling pathways are involved in cell development, embryogenesis, differentiation, and tumorigenesis [35]. Ma *et al.* [36] reported that autophagy and Wnt/β-catenin signaling pathways are upregulated in hepatic progenitor cells (HPCs), which may result in hepatic differentiation of HPCs, and downregulated autophagy can inhibit the Wnt/β-catenin signaling pathway. Chen *et al.* [37] demonstrated that rapamycin-mediated autophagy can inhibit GSK3β, thereby increasing β-catenin expression, which can promote neural differentiation and alleviate Alzheimer's disease symptoms. In this study, we verified that MFAP2 can positively regulate autophagy to promote the viability, proliferation, invasion, and migration of OSCC. Likewise, a similar effect was detected after activating the Wnt/β-catenin signaling pathway by upregulating *MFAP2*. Therefore, our results suggested that both autophagy and Wnt/β-catenin signaling are involved in OSCC development. Moreover, rapamycin reversed the effects of downregulating the Wnt/β-catenin signaling pathway by downregulating MFAP2. Thus, we determined that Wnt/β-catenin signaling mediates MFAP2's contribution to cell proliferation and metastasis via MFAP2-modulated autophagy in OSCCC. Taken together, MFAP2 serves as a positive regulator of both autophagy and Wnt/β-catenin signaling in OSCC. Importantly, MFAP2 can influence OSCC progression by regulating Wnt/β-catenin signaling via autophagy (Figure 7). Until now, studies on the relationship between MFAP2 and autophagy have been very limited, which is one of the motivations for this study. In this study, we confirmed that MFAP2 could affect OSCC by regulating autophagy. Although the exact mechanisms by which MFAP2 regulates autophagy remain unknown, a potential mechanism could be proposed. We performed Kyoto Encyclopedia of Genes and Genomes (KEGG) analysis based on the TCGA dataset, and the results indicated that MFAP2 might be associated with the mTOR signaling pathway and regulate autophagy (Supplementary Figure S2). Further molecular mechanisms should be investigated.

In conclusion, MFAP2 was verified to be upregulated in OSCC tissues and cells, and it was implicated in SCC15 cell malignant behavior, including proliferation, apoptosis, migration, and invasion. Importantly, MFAP2 could serve as a positive regulator of autophagy and Wnt/β-catenin signaling, through which it promotes OSCC tumorigenesis and development. MFAP2 could serve as a novel biomarker and therapeutic target in OSCC.

Supplementary Data

Supplementary data is available at *Acta Biochimica et Biophysica Sinica* online.

Funding

This work was supported by the grants from the National Natural Science Foundation of China (Nos. 31971106, BWS21L013, 18CXZ044, and 21WS09002).

Conflict of Interest

The authors declare that they have no conflict of interest.

References

1. Shield KD, Ferlay J, Jemal A, Sankaranarayanan R, Chaturvedi AK, Bray F, Soerjomataram I. The global incidence of lip, oral cavity, and pharyngeal cancers by subsite in 2012. *CA Cancer J Clin* 2017, 67: 51–64
2. Kumar M, Nanavati R, Modi TG, Dobariya C. Oral cancer: Etiology and risk factors: A review. *J Can Res Ther* 2016, 12: 458–463
3. Ferlay J, Colombet M, Soerjomataram I, Mathers C, Parkin DM, Piñeros M, Znaor A, *et al.* Estimating the global cancer incidence and mortality in 2018: GLOBOCAN sources and methods. *Int J Cancer* 2019, 144: 1941–1953
4. Zhu S, Ye L, Bennett S, Xu H, He D, Xu J. Molecular structure and function of microfibrillar-associated proteins in skeletal and metabolic disorders and cancers. *J Cell Physiol* 2021, 236: 41–48
5. Henderson M, Polewski R, Fanning JC, Gibson MA. Microfibril-associated glycoprotein-1 (MAGP-1) is specifically located on the beads of the beaded-filament structure for fibrillin-containing microfibrils as visualized by the rotary shadowing technique. *J Histochem Cytochem* 1996, 44: 1389–1397

6. Villain G, Lelievre E, Broekelmann T, Gayet O, Havet C, Werkmeister E, Mecham R, *et al.* MAGP-1 and fibronectin control EGFL 7 functions by driving its deposition into distinct endothelial extracellular matrix locations. *FEBS J* 2018, 285: 4394–4412
7. Qiu Z, Xin M, Wang C, Zhu Y, Kong Q, Liu Z. Pan-cancer analysis of microfibrillar-associated protein 2 (MFAP2) based on bioinformatics and qPCR verification. *J Oncol* 2022, 2022: 8423173
8. Turecamo SE, Walji TA, Broekelmann TJ, Williams JW, Ivanov S, Wee NK, Procknow JD, *et al.* Contribution of metabolic disease to bone fragility in MAGP1-deficient mice. *Matrix Biol* 2018, 67: 1–14
9. Chen Z, Lv Y, Cao D, Li X, Li Y. Microfibril-associated protein 2 (MFAP2) potentiates invasion and migration of melanoma by EMT and wnt/β-catenin pathway. *Med Sci Monit* 2020, 26: e923808
10. Wang JK, Wang WJ, Cai HY, Du BB, Mai P, Zhang LJ, Ma W, *et al.* MFAP2 promotes epithelial-mesenchymal transition in gastric cancer cells by activating TGF-β/SMAD2/3 signaling pathway. *Onco Targets Ther* 2018, 11: 4001–4017
11. Betin VMS, Singleton BK, Parsons SF, Anstee DJ, Lane JD. Autophagy facilitates organelle clearance during differentiation of human erythroblasts. *Autophagy* 2013, 9: 881–893
12. Stefater JA 3rd, Rao S, Bezold K, Aplin AC, Nicosia RF, Pollard JW, Ferrara N, *et al.* Macrophage Wnt-Calcineurin-Flt1 signaling regulates mouse wound angiogenesis and repair. *Blood* 2013, 121: 2574–2578
13. Cai X, Yao Z, Li L, Huang J. Role of DKK4 in tumorigenesis and tumor progression. *Int J Biol Sci* 2018, 14: 616–621
14. Alamoud KA, Kukuruzinska MA. Emerging insights into wnt/β-catenin signaling in head and neck cancer. *J Dent Res* 2018, 97: 665–673
15. Sha J, Han Q, Chi C, Zhu Y, Pan J, Dong B, Huang Y, *et al.* Upregulated KDM4B promotes prostate cancer cell proliferation by activating autophagy. *J Cell Physiol* 2020, 235: 2129–2138
16. Wang Y, Wang Y, You F, Xue J. Novel use for old drugs: the emerging role of artemisinin and its derivatives in fibrosis. *Pharmacol Res* 2020, 157: 104829
17. Fan Y, Hou T, Dan W, Liu T, Luan J, Liu B, Li L, *et al.* Silibinin inhibits epithelial mesenchymal transition of renal cell carcinoma through autophagy dependent Wnt/β catenin signaling. *Int J Mol Med* 2020, 45: 1341–1350
18. Chen L, Yang Y, Bao J, Wang Z, Xia M, Dai A, Tan J, *et al.* Autophagy negative-regulating Wnt signaling enhanced inflammatory osteoclastogenesis from Pre-OCs in vitro. *Biomed Pharmacother* 2020, 126: 110093
19. Turcios L, Chacon E, Garcia C, Eman P, Cornea V, Jiang J, Spear B, *et al.* Autophagic flux modulation by Wnt/β-catenin pathway inhibition in hepatocellular carcinoma. *PLoS ONE* 2019, 14: e0212538
20. Ferlay J, Soerjomataram I, Dikshit R, Eser S, Mathers C, Rebelo M, Parkin DM, *et al.* Cancer incidence and mortality worldwide: Sources, methods and major patterns in GLOBOCAN 2012. *Int J Cancer* 2015, 136: E359–E386
21. Petherick KJ, Williams AC, Lane JD, Ordóñez-Morán P, Huelsken J, Collard TJ, Smartt HJ, *et al.* Autolysosomal β-catenin degradation regulates Wnt-autophagy-p62 crosstalk. *EMBO J* 2013, 32: 1903–1916
22. Panda PK, Naik PP, Praharaj PP, Meher BR, Gupta PK, Verma RS, Maiti TK, *et al. Abrus* agglutinin stimulates BMP-2-dependent differentiation through autophagic degradation of β-catenin in colon cancer stem cells. *Mol Carcinogenesis* 2018, 57: 664–677
23. Gómez de Segura I, Ahechu P, Gómez-Ambrosi J, Rodríguez A, Ramírez B, Becerril S, Unamuno X, *et al.* Decreased levels of microfibril-associated glycoprotein (magp)-1 in patients with colon cancer and obesity are associated with changes in extracellular matrix remodelling. *Int J Mol Sci* 2021, 22: 8485
24. Sun T, Wang D, Ping Y, Sang Y, Dai Y, Wang Y, Liu Z, *et al.* Integrated profiling identifies SLC5A6 and MFAP2 as novel diagnostic and prognostic biomarkers in gastric cancer patients. *Int J Oncol* 2020, 56: 460–469
25. Yao L, Wu L, Zhang L, Zhou W, Wu L, He K, Ren J, *et al.* MFAP2 is overexpressed in gastric cancer and promotes motility via the MFAP2/integrin α5β1/FAK/ERK pathway. *Oncogenesis* 2020, 9: 17
26. Li X, He S, Ma B. Autophagy and autophagy-related proteins in cancer. *Mol Cancer* 2020, 19: 12
27. Song B, Bian Q, Zhang YJ, Shao CH, Li G, Liu AA, Jing W, *et al.* Downregulation of ASPP2 in pancreatic cancer cells contributes to increased resistance to gemcitabine through autophagy activation. *Mol Cancer* 2015, 14: 177
28. Marsh T, Debnath J. Autophagy suppresses breast cancer metastasis by degrading NBR1. *Autophagy* 2020, 16: 1164–1165
29. Peng L, Sang H, Wei S, Li Y, Jin D, Zhu X, Li X, *et al.* circCUL2 regulates gastric cancer malignant transformation and cisplatin resistance by modulating autophagy activation via miR-142-3p/ROCK2. *Mol Cancer* 2020, 19: 156
30. Khan T, Relitti N, Brindisi M, Magnano S, Zisterer D, Gemma S, Butini S, *et al.* Autophagy modulators for the treatment of oral and esophageal squamous cell carcinomas. *Med Res Rev* 2020, 40: 1002–1060
31. Xie Y, Wang B. Downregulation of TNFAIP2 suppresses proliferation and metastasis in esophageal squamous cell carcinoma through activation of the Wnt/β-catenin signaling pathway. *Oncol Rep* 2017, 37: 2920–2928
32. Robinson JA, Chatterjee-Kishore M, Yaworsky PJ, Cullen DM, Zhao W, Li C, Kharode Y, *et al.* Wnt/β-catenin signaling is a normal physiological response to mechanical loading in bone. *J Biol Chem* 2006, 281: 31720–31728
33. Nusse R, Clevers H. Wnt/β-catenin signaling, disease, and emerging therapeutic modalities. *Cell* 2017, 169: 985–999
34. Zhang Y, Wang X. Targeting the Wnt/β-catenin signaling pathway in cancer. *J Hematol Oncol* 2020, 13: 165
35. Lorzadeh S, Kohan L, Ghavami S, Azarpira N. Autophagy and the Wnt signaling pathway: a focus on Wnt/β-catenin signaling. *Biochim Biophys Acta* 2021, 1868: 118926
36. Ma Z, Li F, Chen L, Gu T, Zhang Q, Qu Y, Xu M, *et al.* Autophagy promotes hepatic differentiation of hepatic progenitor cells by regulating the Wnt/β-catenin signaling pathway. *J Mol Hist* 2019, 50: 75–90
37. Chen J, Long Z, Li Y, Luo M, Luo S, He G. Alteration of the Wnt/GSK3β/β catenin signalling pathway by rapamycin ameliorates pathology in an Alzheimer's disease model. *Int J Mol Med* 2019, 44: 313–323